

Characteristics of Sn8Zn3Bi solder joints and crack resistance with various PCB and lead coatings

Young Woo Lee ^a, Ki Ju Lee ^a, Y. Norman Zhou ^b, Jae Pil Jung ^{a,*}

^a Department of Materials Science and Engineering, University of Seoul, Seoul 130-743, Republic of Korea

^b Department of Mechanical Engineering, University of Waterloo, Waterloo, Canada N2L 3G1

Received 26 May 2007; received in revised form 1 September 2007

Available online 11 December 2007

Abstract

Reliability of QFP (quad flat package) solder joints after thermal shock was investigated for PCB's and connecting leads plated with several different alloy coatings before soldering. Sn–8 wt%Zn–3 wt%Bi (hereafter, Sn–8Zn–3Bi) was selected as a solder, and FR-4 PCB's finished with Cu/Sn, Cu/OSP and Cu/Ni/Au were used as substrates. The leads of the QFP were Cu plated with Sn–10 wt%Pb, or Sn, or Sn–3 wt%Bi. The QFP chips were mounted on the substrates using a Sn–8Zn–3Bi solder paste and reflowed in air atmosphere. The pull strength and microstructure for the soldered leads of QFP were evaluated before and after thermal shock testing. The leads plated with Sn or Sn–3Bi showed approximately 40–50% higher pull strength than the reference value of a Sn–37%Pb solder joint for all PCB-finishes. However, in the case of leads coated with Sn–10Pb, the pull strength of the leads soldered to a Sn-finished PCB was 21% lower than the reference value. In microstructure analysis of the joints with Sn–10Pb-plated leads, cracks were found along the bonded interface for Sn-finished PCB. The cracks were believed to start from the low melting temperature phase, 49.38 wt% Pb–32.58 wt%Sn–18.03 wt%Bi, found around the crack, and then propagated through Cu–Zn intermetallic compound. Meanwhile, even when using Sn–10Pb-plated leads, the PCB's finished with Cu/Ni/Au coating had about 30% higher strength than the reference value, and cracks were hardly found on the soldered joint. Thus, even with Sn–10Pb-plated leads the Cu/Ni/Au-finished PCB's were evaluated to be as reliable as the reference joint.

© 2007 Elsevier Ltd. All rights reserved.

1. Introduction

In the electronic industry, Pb-bearing solders are restricted in use because of environmental concerns. Numerous Pb-free solders have been investigated to replace conventional Pb-bearing solders, and Sn–Ag–Cu, Sn–Ag–Bi, Sn–Zn–Bi and Sn–Cu based alloys are popular candidates [1]. Especially Sn–Ag–Cu alloy is a leading candidate [2] because of its high reliability and solderability. However, high melting point and high cost are drawbacks of this solder.

Meanwhile, Sn–8Zn–3Bi solder has several advantages such as a melting point (around 197 °C) that is much closer to Sn–37%Pb, good mechanical properties and low price.

Considering the mechanical properties of Sn–Zn based alloys, Iwanishi et al. [3] reported that thermal shock resistance of soldered joints between –40 and 125 °C was better than that of Sn–37Pb. In the case of the quad flat package (QFP), the bond strength of a Sn–Zn alloy after aging at 125 °C for 2000 h, where its leads were plated with Sn–Bi before soldering, was equal to or higher than that of Sn–37Pb [4]. During a thermal shock test, the acicular shaped Zn phase is known to be changed to a round shape although this change has not been found to cause drastic strength decrease [5].

Furthermore, study of solderability of various combinations of platings on electronic parts and on PCB pads is important for practical application of Sn–8Zn–3Bi solder. A study has been reported of the aging properties of Sn–8Zn–3Bi solder joints with various lead plating but with a single plated finish coating on the PCB pads [6]. In this

* Corresponding author. Tel.: +82 2 2210 2981; fax: +82 2 2215 5863.
E-mail address: jjjung@uos.ac.kr (J.P. Jung).

work, properties of soldered joints with various combinations of lead plating on QFP chips and different PCB-finishes were studied, including thermal shock resistance and the presence of low melting point phases.

2. Experimental

For soldering experiments, printed circuit boards (PCB's) of type FR-4 were used as a substrate, and quad flat package chips (QFP) as a soldering sample. Size of the PCB's was $150 \times 120 \times 1.6(t)$ mm, and the metal pads on the PCB's were composed of Cu/Sn, Cu/OSP (organic solderability preservative) or Cu/Ni/Au from bottom to top. The Sn-layer (thickness; $0.45 \mu\text{m}$) was plated by immersion method, and Ni was electroless-plated (thickness; $3 \mu\text{m}$) and Au was electroplated (thickness; $0.03 \mu\text{m}$). The QFP soldering sample had 208 pins with a pitch of 0.5 mm. The leads were Cu, and on the lead surface Sn–10 wt%Pb, or Sn, or Sn–3 wt%Bi were plated with a thickness of $7.6 \mu\text{m}$.

Composition of the solder was Sn–8 wt%Zn–3 wt%Bi (hereafter, Sn–8Zn–3Bi), and the solder paste was printed on the PCB pads using a stencil with a thickness of 0.15 mm. The QFP was mounted on the PCB coated with printed paste, and reflow soldered. The peak soldering temperature was in the range of $215\text{--}225 \text{ }^\circ\text{C}$, and holding temperature above the melting point of the solder was $65\text{--}75 \text{ s}$. In order to provide a comparison with the Sn–8Zn–3Bi solder joint, a reference sample was also prepared. The reference consisted of Sn–37 wt%Pb solder, OSP-finished PCB pads, and leads plated with Sn–15%Pb.

For the solder joints of the QFP, thermal shock testing was performed between $-40 \text{ }^\circ\text{C}$ and $85 \text{ }^\circ\text{C}$, holding 30 min at each peak temperature. The number of thermal cycles reached 1000 and after every 200 cycles microstructure and pull strength of the solder joints were estimated. During the pull test of the lead, the angle between the hook and the PCB was 45° . Total number of leads pull tested was 80 for each soldering condition. Microstructure was examined by FESEM (field emission scanning electron microscopy), and the chemical composition of IMC (intermetallic compound(s)) was analyzed by EDS (energy dispersive spectrometer) and EPMA (electron probe X-ray micro analyzer).

3. Results and discussion

3.1. Pull strength and microstructure

Fig. 1 shows the pull strength data of the QFP solder joints as a function of thermal shock cycles. For all PCB finishes and all lead plating compositions, the pull strengths remained nearly constant with accumulated thermal cycles. On the OSP- and Ni/Au-finished PCB's, the pull strength of leads plated with Sn or Sn–3Bi showed similar values, although the latter was slightly stronger. From these results, Sn or Sn–3Bi plating gave approximately 30–

50% higher pull strength than the reference solder joint of Sn–37Pb, i.e., about 9.5 N.

For the OSP- and Sn-finished PCB's, the Sn–10Pb-plated leads had lower strengths (see Fig. 1a and b). Especially in the case of Sn-finish, the Sn–10Pb plating showed the lowest strength, around 7.5 N, and about 53% lower than those of other lead plating compositions of 15–16 N, and even lower than the reference values. However, in case of Ni/Au-finished PCB (Fig. 1c), the strength of Sn–10Pb-plated lead was closer to those of the other two platings of Sn and Sn–3Bi, and approximately 30% higher than the reference value obtained with Sn–37%Pb solder. From the results shown in Fig. 1, it was found that the Sn–8Zn–3Bi solder when used on Ni/Au finished PCB's gave joint strengths superior to those obtained with Sn–37%Pb solder, for all lead plating compositions employed.

Fig. 2 shows the cross sections of the solder joints in as-soldered state. The leads plated with Sn or Sn–3Bi provided sound joints without cracks for all PCB's. On the other hand, in the case of leads plated with Sn–10Pb, cracking was observed in the as-soldered state for Sn-finished PCB. This defect was believed to be solidification crack, and the crack was expected to decrease the pull strength, as actually shown in Fig. 1b. However, when the Ni/Au-finished PCB's were used cracks were hardly found, and the pull strength had about 30% higher average than the reference value.

Generally Cu_6Sn_5 and Ni_3Sn_4 intermetallics are produced on Cu- and Ni-pads, respectively, in soldering with most Sn-based solder. However, in the case of Sn–Zn solder, Cu reacts with Zn instead of with Sn. Thus, Cu–Zn compounds such as Cu_5Zn_8 , and Ni–Zn compounds like $\text{Ni}_5\text{Zn}_{21}$ are produced on Cu- and on Ni-pads, respectively, when using Sn–Zn based solder [7–9]. Cu_5Zn_8 has lower Gibbs free energy than Cu_6Sn_5 specifically -12.10 and -6.26 kJ/mol at $150 \text{ }^\circ\text{C}$, respectively, and thus Cu_5Zn_8 is found to be more stable between Cu and Sn–Zn based solder [10]. The Cu_5Zn_8 is also known as a stable phase after thermal cycling compared to CuZn or CuZn_2 which has been shown to disappear after aging at $130 \text{ }^\circ\text{C}$ for 20 h [11] or after 3 thermal cycles [10] between -30 and $150 \text{ }^\circ\text{C}$, respectively.

Fig. 3 shows interfacial IMCs formed between QFP leads with different plated surfaces and Sn–8Zn–3Bi solder after 1000 cycles of thermal shock. The composition of the Cu–Zn IMC on the Sn–10Pb-plated lead was confirmed as 37.51 at%Cu–53.74 at%Zn–8.75 at%Sn, and other interfacial IMCs produced between Sn and Sn–3Bi plating showed similar compositions. This IMC is believed to be Cu_5Zn_8 containing some Sn, and similar IMCs were reported by other researchers [12,13]. In the case of Sn–10Pb plating, small cracks were also observed at the bonded interface.

Interfaces between solder and PCB-pads are illustrated in Fig. 4. IMCs formed on OSP- and Sn-finished pads were similar to that shown in Fig. 3, i.e., Cu_5Zn_8 . However, in

the case of Ni/Au-finished pads, the chemical composition of the IMC at point ‘a’ was confirmed as 18.21 at%Ni–67.47 at%Zn–14.32 at%Sn. In this case, differently from

the observation on OSP- and Sn-finished pads, Cu was located under the Ni-layer, and thus was not incorporated in the IMC.

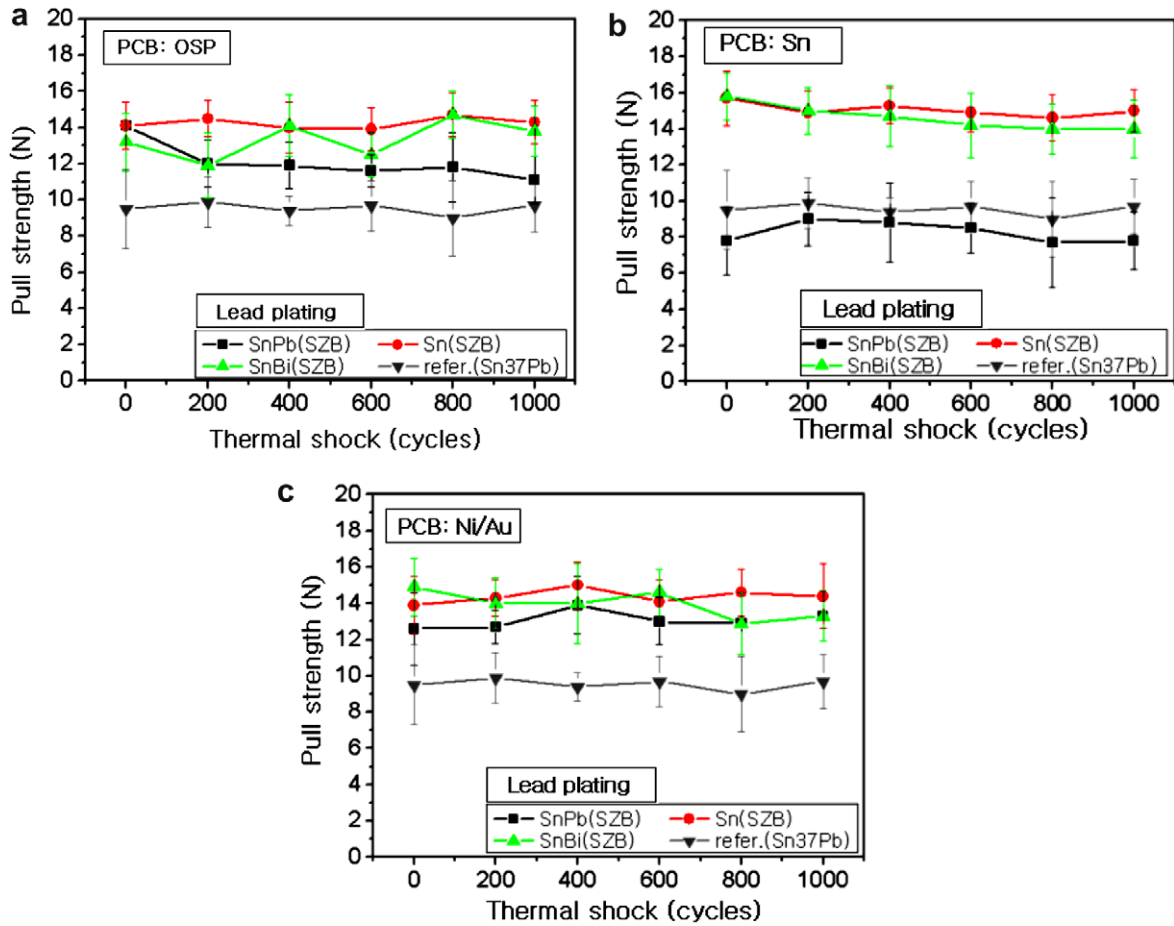


Fig. 1. Pull strength of the QFP leads after TS (thermal shock) test (–45/85 °C) (a) OSP-finished PCB, (b) Sn-finished PCB, (c) Ni/Au-finished PCB.

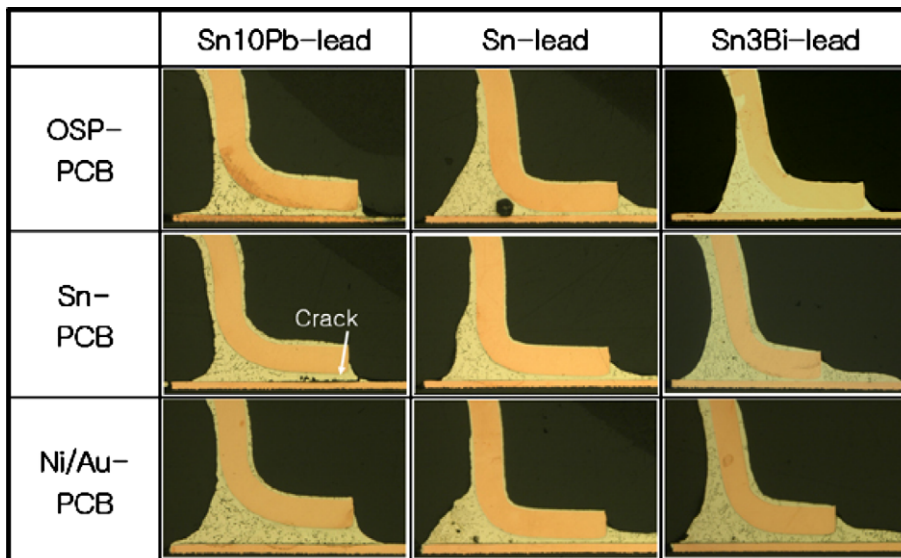


Fig. 2. Cross-sections of the as-soldered state of QFP with Sn–8Zn–3Bi solder.

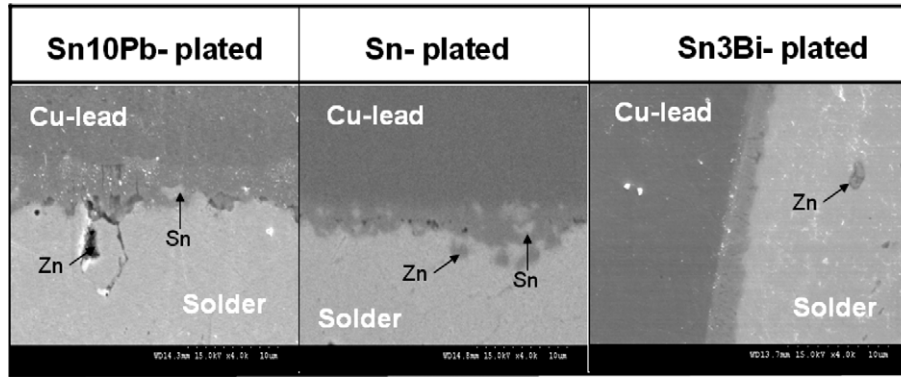


Fig. 3. Interfaces between Sn–8Zn–3Bi solder and leads with different plating after thermal shock testing ($-40/85^{\circ}\text{C}$, 1000 cycles).

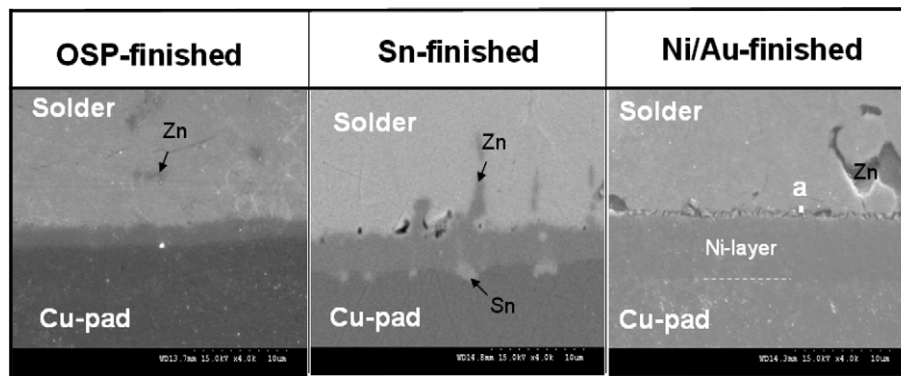


Fig. 4. Interfaces between Sn–8Zn–3Bi solder and PCB-pads with different plating after thermal shock testing ($-40/85^{\circ}\text{C}$, 1000 cycles).

3.2. Low melting temperature phase and cracking

For the Sn-finished pads, the leads plated with Sn–10Pb showed lower bond strength than the reference value due to cracks. In order to investigate these cracks in more detail, EDS and EPMA analyses were performed. Fig. 5 shows the result of EPMA analysis for a joint between Sn–

10Pb-plated lead and Sn-plated pad after 200 thermal cycles. As shown in Fig. 5 some round phases were produced around the crack (see points 'a' and 'b'). Their compositions were confirmed as 49.38 wt% Pb–32.58 wt%Sn–18.03 wt%Bi (point a), 51.64 wt% Pb–24.92 wt%Sn–23.43 wt%Bi (point b) by EPMA. It has previously been pointed out that Sn, Pb and Bi can produce a low melting

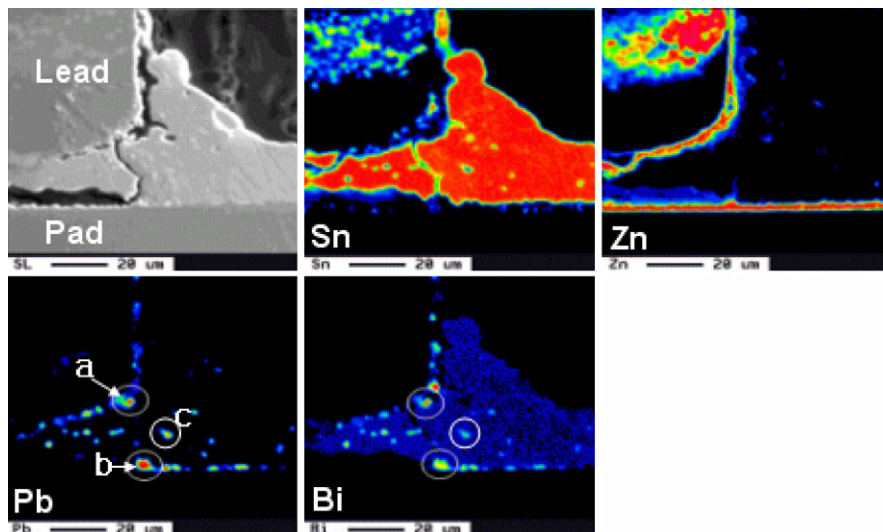


Fig. 5. Low temperature phase observed in the Sn–8Zn–3Bi joints between Sn–10Pb-plated leads and Sn-plated PCB after 200 cycles of TS test.

temperature phase [14]. For example, 43 wt%Pb–28.5 wt%Bi–28.5 wt%Sn [15] has solidus and liquidus at 95 °C and 137 °C, respectively. Other alloys such as 50 wt%Pb–30 wt%Sn–20 wt%Bi produced from the Indium Co., which is a closer composition to point ‘a’ and ‘b’ of Fig. 5, has a melting range of 130–173 °C [15]. Thus the phases observed evidently had a melting temperature well below that of the solder itself, 197 °C. Specifically, during solidification of the Sn–8Zn–3Bi, this low melting temperature phase exists as a liquid below the solder’s melting temperature. Thermal and solidification shrinkage could readily make the residual liquid Pb–Sn–Bi phase be torn to produce a crack. Cracking was observed along the bonded interface where the Pb–Sn–Bi phase was found (see Fig. 5). However, the Pb–Sn–Bi phase was also seen inside the bulk solder such as at point ‘c’ and there it did not produce any cracking.

The EDS results for the Sn–10Pb leads soldered on pads with Ni/Au-finish are shown in Fig. 6. In this mate-

rial combination, cracking was hardly found, and average lead pull strength was 30% higher than the reference value as shown in Fig. 1c. On the Ni/Au-pads, the Sn, Pb and Bi were much less segregated compared to the behavior on Sn-plated pads (see Fig. 6). Meanwhile, Au dissolved from the pad can produce Au–Pb intermetallics such as AuPb₃, AuPb₂ or Au₂Pb [16,17] with dissolved Pb from the lead above 212.5 °C. Au also can produce Au₂Bi between Bi from the solder, although this decomposes to (Au) and (Bi) below 116 °C [18]. These apparently could suppress the production of low melting temperature phases of Pb–Sn–Bi and cracks, which resulted in the strength increase. Additionally, on the Ni/Au-finished pads, a Ni–Zn IMC of type Ni₅Zn₂₁ was produced along the pad interface, which is different from the Cu₅Zn₈ seen on the Cu/Sn- and Cu/OSP-finished pads. The difference in coefficient of thermal expansion (CTE) of the two IMCs, Ni₅Zn₂₁ versus Cu₅Zn₈, could also affect crack generation.

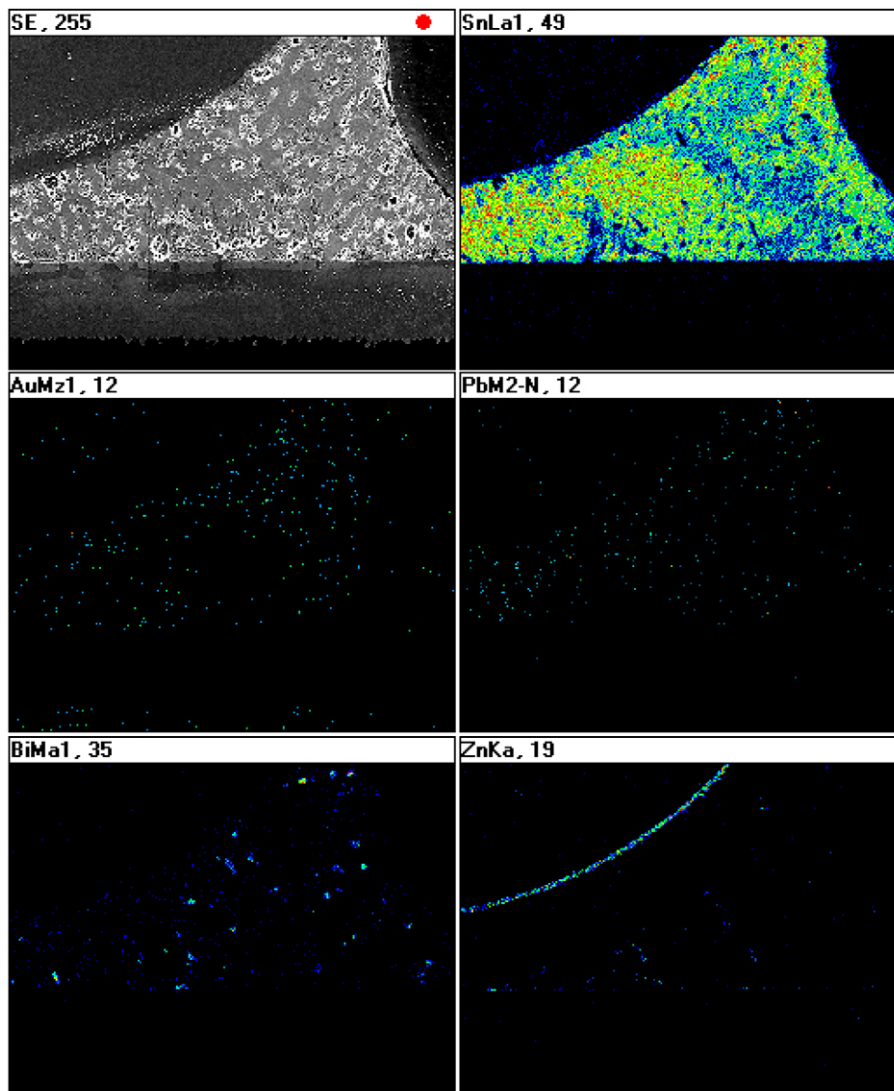


Fig. 6. Cross section of a Sn–8Zn–3Bi joint between Sn–10Pb-plated lead and Ni/Au-plated PCB.

Small cracks produced around a bonded interface can propagate by thermal stress during thermal cycling. Fig. 7 shows a typical crack path, and the composition adjacent to crack path was analyzed by EDS. Along both

sides of the crack, Cu–Zn IMC of type Cu_5Zn_8 was observed, which indicates that Cu_5Zn_8 was acting as a crack path. The Cu_5Zn_8 has been reported as a crack path during thermal cycling in Sn–9Zn solder joints by Chang

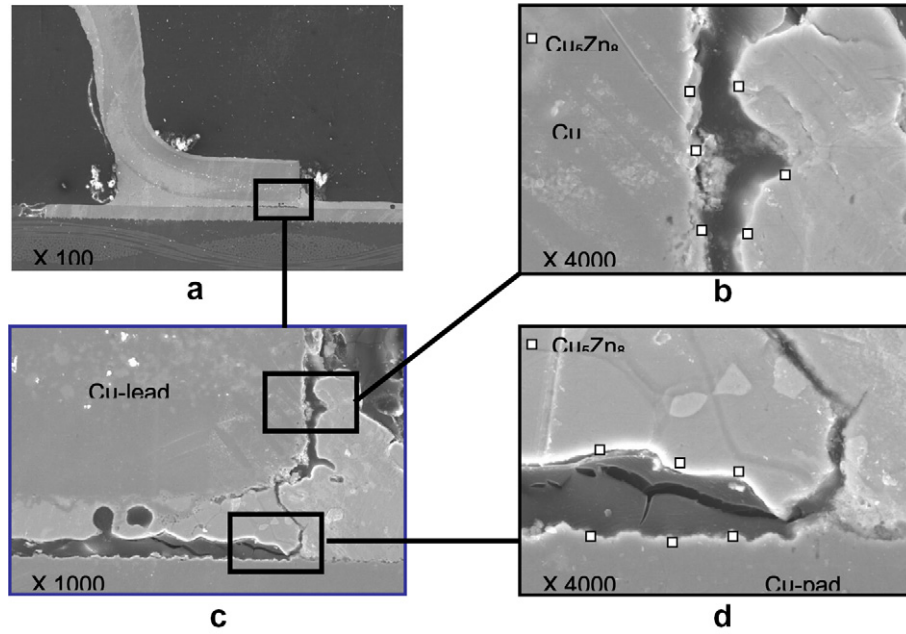


Fig. 7. Crack propagation along IMC of the Sn–8Zn–3Bi joint from Fig. 8.

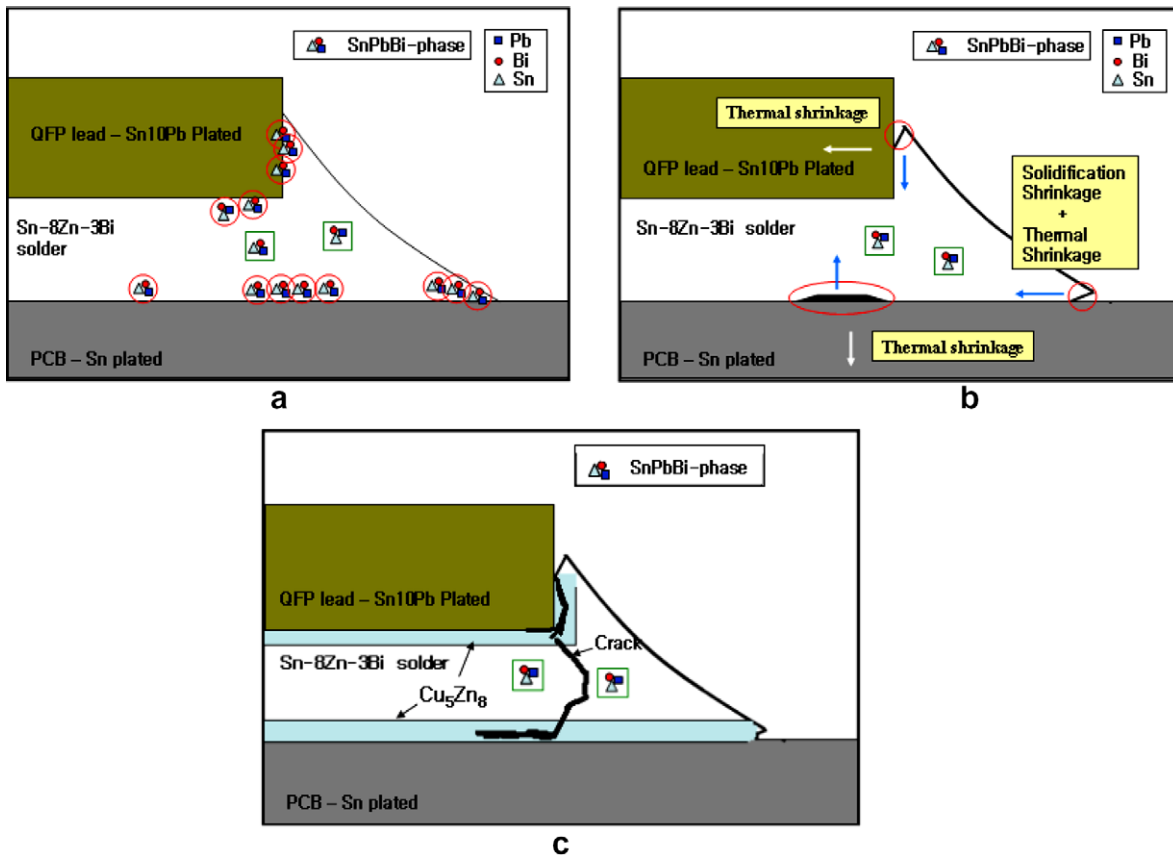


Fig. 8. Formation and growth sequence of cracks initiated by low-temperature phase.

et al. [10]. In that work, cracks were propagated along Sn–9Zn solder and Cu_5Zn_8 interfaces by applying five thermal cycles between -30 and 150 °C. The cracking was suggested to be due to inferior bonding strength between Sn–9Zn solder and Cu_5Zn_8 , and thermal stress during the thermal cycles.

From the above results, the cracking phenomenon in the joints between Sn–8Zn–3Bi and Sn–10Pb-plated leads can be explained as shown in Fig. 8. Specifically, Pb dissolved from the lead surface and combined with Sn–Bi in the solder to form low melting temperature phases such as 49.38 wt% Pb–32.58 wt%Sn–18.03 wt%Bi and 51.64 wt% Pb–24.92 wt%Sn–23.43 wt%Bi (Fig. 8a). During solidification of the solder joint, small cracks were produced by thermal and solidification shrinkages by tearing through the liquid films of Pb–Sn–Bi phase (Fig. 8b). The small cracks then propagated during thermal cycling through the brittle Cu–Zn intermetallics due to thermal stress.

4. Conclusions

Sn–8 wt%Zn–3 wt%Bi solder joints with various combinations of PCB-finish and QFP lead-plating were investigated. The plating on Cu leads was Sn–10 wt%Pb, Sn, or Sn–3 wt%Bi and PCB-finish was OSP, Sn or Ni/Au on Cu pads. Pull strength before and after thermal shock treatment was characterized. A low melting temperature phase found in some joints was investigated. The results are as follows:

1. Sn-finished PCB's soldered to Sn–10Pb plated leads gave around 20% lower strength than the reference value of Sn–37Pb solder joints, due to cracking along the joints.
2. Cracks were initiated due to formation of a low melting temperature phase such as 49.38 wt% Pb–32.58 wt%Sn–18.03 wt%Bi, and they propagated through a Cu–Zn IMC layer along the bonded interface.
3. The Ni/Au-finished PCB's could suppress cracking in the solder joints even when using the Sn–10Pb plated leads, and showed 30% higher strength than Sn–37%Pb. In this joint Sn, Pb and Bi were less segregated and phases associated with low melting temperature were virtually not observed.
4. The leads plated with Sn or Sn–3Bi showed approximately 30–50% higher pull strength on all compositions of PCB pad finish than the reference value of Sn–37Pb solder joints. The pull strengths remained nearly constant after thermal cycling for most combinations of surface platings.

Acknowledgement

This study was financially supported by the Ministry of Commerce, Industry & Energy, and Samsung Electronics, Korea.

References

- [1] Hirose A, Yanagawa H, Ide E, Kobayashi KF. Joint strength and interfacial microstructure between Sn–Ag–Cu and Sn–Zn–Bi solders and Cu substrate. *Sci Technol Adv Mater* 2004;5:267–76.
- [2] Zhong WH, Chan YC, Alam MO, Wu BY, Guan JF. Effect of multiple reflow processes on the reliability of ball grid array (BGA) solder joints. *J Alloys Compd* 2006;414:123–30.
- [3] Iwanishi H, i Imamura T, Hirose A, Kobayashi KF, Tateyama K, Mori I. Effect of Lead Plating Materials on Properties of QFP Joints Using Sn–Zn–Bi Solder. In: 8th Symposium on MATE; 2002: p. 277–82.
- [4] Amita H, Murase N, Sibuya Y, Nagasaki S, Shoji T. Development of Pb-free Solder Paste in Sn–Zn Alloy System for the Air Reflow. In: 6th Symposium on MATE; 2000: p. 319–24.
- [5] Hisazato Y, Kato M, Kawakami K, Saito Y. Reliability Assessment of Sn–Ag and Sn–Zn Lead Free Solder Joints by Thermal Fatigue. In: 9th Symposium on MATE; 2003: p. 339–44.
- [6] Iwanishi H, Imamura T, Hirose A, Tateyama K, Mori I, Kobayashi KF. Properties of quad flat package joints using Sn–Zn–Bi solder with varying lead-plating materials. *J Electron Mater* 2003;32(12): 1540–6.
- [7] Shohji Ikuo, Nakamura Takao, Mori Fuminari, Fujiuchi Shinichi. Interface reaction and mechanical properties of lead-free Sn–Zn alloy/Cu joints. *Mater Trans* 2002;43:1797–801.
- [8] Chiu MY, Wang SS, Chuang TH. Intermetallic compounds formed during interfacial reactions between liquid Sn–8Zn–3Bi solders and Ni substrates. *J Electron mater* 2002;31(5):494–9.
- [9] Ichitsubo T, Matsubara E, Fujiwara K, Yamaguchi M, Irie H, Kumamoto S, et al. Control of compound forming reaction at the interface between SnZn solder and Cu substrate. *J Alloys Compd* 2005;392:200–5.
- [10] Chang T, Hon M, Wang M, Lin D. Thermal fatigue resistance of the Sn–9Zn–xAg lead-free solders/Cu interface. In: *IEEE Int'l Sympo On Electronic Mater Pack*; 2002: p. 307–12.
- [11] Mei Z et al. Analysis of low-temperature intermetallic growth in copper-tin diffusion couples. *Metall Trans A* 1992;23:854–7.
- [12] Abe Takeshi, Sawada Shoji, Maeda Akira. Interface reaction of the Sn–8Zn–3Bi Solder. In: 8th Symposium on MATE; 2002: p. 283–8.
- [13] Ikeda Haruhiko, Kamada Nobuo. Interface reaction of the Sn–8Zn–3Bi Solder and Cu Electrode. In: 7th Symposium on MATE; 2001: p. 487–90.
- [14] Yoon SW, Lee HM. A thermodynamic study of phase equilibria in the Sn–Bi–Pb solder system. *Calphad* 1998;22(2):167–78.
- [15] Mei Zequn, Hua Fay, Judy Glazer. Low Temperature Soldering. In: *IEEE/CPMT Int'l Electronics Manufacturing Technology Symposium*; 1997: p. 463–76.
- [16] Wang J, Liu HS, Jin ZP. Thermodynamic assessment of the Au–Pb system. *Comp Coupling Phase Diagrams Thermochem* 2004;28: 91–95.
- [17] Okamoto H, Massalski TB. Binary alloy phase diagram; 1984. p. 293.
- [18] Okamoto H, Massalski TB. Binary alloy phase diagram; 1984. p. 239.